Eur. Phys. J. A **1**, 399–406 (1998)

THE EUROPEAN PHYSICAL JOURNAL A

Time-scale and excitation energy partition in sequential binary decays induced by heavy-ion collisions at $\simeq 6$ MeV·A

P. Boccaccio[1], L. Vannucci[1], R.A. Ricci[1,2], G. Vannini[3,4], R. Dona[5,6], I. Massa[5,6], J.P. Coffin[7], P. Fintz[7], G. Guillaume[7], F. Jundt[7], F. Rami[7], P. Wagner[7]

[1] Istituto Nazionale di Fisica Nucleare, Laboratori Nazionali di Legnaro, I-35020 Legnaro, Italy
[2] Dipartimento di Fisica dell'Universita'di Padova, I-35100 Padova, Italy
[3] Dipartimento di Fisica dell'Universita' di Trieste, I-34100 Trieste, Italy,
[4] Istituto Nazionale di Fisica Nucleare, Sezione di Trieste, I-34100 Trieste, Italy
[5] Dipartimento di Fisica dell'Universita' di Bologna, I-40100 Bologna, Italy,
[6] Istituto Nazionale di Fisica Nucleare, Sezione di Bologna, I-40100 Bologna, Italy
[7] Centre de Recherches Nucleaires, Universite' Louis Pasteur, F-67037 Strasbourg, France

Received: 25 March 1997 / Revised version: 2 December 1997
Communicated by C. Signorini

Abstract. We studied the sequential binary decay of the systems ^{32}S+^{45}Sc, ^{76}Ge, ^{89}Y, ^{59}Co, ^{63}Cu and ^{19}F+^{63}Cu induced by collisions at $\simeq 6$ MeV·A. The two stages of the process have reaction-times compatible with the dynamics of different mechanisms. The study of the excitation energy partition shows that the reaction mechanism of the first step has influence on the de-excitation of the primary fragments producing two decay components which have different time scale.

PACS. 25.70.Ef Resonances

1 Introduction

An important and still open question, concerning dissipative reactions induced by heavy ion collisions, is related to the excitation energy partition between the produced fragments.

Early studies of deep-inelastic reactions suggested that the sharing of excitation energy is proportional to the fragment masses [1-5], i.e. the fragments are heated to equal temperature as it is expected if thermal equilibrium is attained. However, some other measurements indicate that the partition of excitation energy between the fragments is nearly equal over a large range of dissipated kinetic energy [6, 7]. Several theoretical models have been developed so far to describe the basic mechanism leading to the observed sharing of the excitation energy. In the framework of the transport theory [8-11], for example, it is assumed that the dissipation of the kinetic energy available in the entrance channel occurs by stochastic exchange of nucleons between the fragments. In this assumption, the excitation energies of the fragments are predicted to be nearly equal for moderate total kinetic energy losses (TKEL), whereas for higher TKEL a transition to the equilibrium energy division is expected.

At low excitation energy the kind of sharing has a relevant influence on decay probability of the primary fragments and then on their life-time. So, in particular at low bombarding energy, the possibility to observe sequential binary processes is ruled out by the dissipation mechanism of the kinetic energy and by the excitation energy partition.

A recent note [12] reports the presence of a sequential binary process in six reactions induced by low-energy collisions ($E_{lab} < 6.5$ MeV·A) in systems of the medium mass region.

For these six reactions (^{32}S+^{45}Sc, ^{76}Ge, ^{89}Y, ^{59}Co, ^{63}Cu and ^{19}F+^{63}Cu) we report in this paper the study of the reaction time-scale and of the excitation energy partition between the two primary fragments that was preliminarly presented in [13].

2 Experimental

The six studied reactions were measured at $\simeq 60$ MeV over the interaction barrier. A first set of measurement was performed at the Centre des Recherches Nucleaires in Strasbourg by using a 180 MeV ^{32}S beam colliding on ^{59}Co ([14]), ^{45}Sc ([15]), ^{76}Ge and ^{89}Y ([12]) targets. Pairs of fragments, produced in the reaction, were detected in coincidence measuring their atomic number (Z_1 and Z_2) and their kinetic energy (E_1 and E_2) by two telescopes ΔE(gas ionization chamber)-E(silicon surface barrier detector, SSB) subtending 6 msr each. The telescopes were placed on the opposite sides of the beam axis at the detection angles $\theta_1 = 25°$ and $\theta_2 = -25°$, $-35° - 45°$; however

only the two largest couples of angles were considered in the analysis. This constraint was due to the mixing, at $\theta_1 = 25°$ and $\theta_2 = -25°$, of three-body events with binary events from reactions on target contaminants (Carbon and Oxygen). The contribution to the yield, of this last kind of events, was evaluated studying the $^{32}S+^{12}C$ and the $^{32}S+Ta_2O_5$ reactions: the experimental results showed that the contamination was important at $\theta_1 = 25°$ and $\theta_2 = -25°$ and negligible at the largest angles.

A second set of reactions [15] ($^{32}S+^{59}Co$, $^{19}F+^{63}Cu$, $^{32}S+^{63}Cu$) was studied at the Laboratori Nazionali di Legnaro by using a 180 MeV ^{32}S and a 120 MeV ^{19}F beam with an apparatus covering a much larger solid angle. The $^{32}S+^{59}Co$ reaction was measured again to ensure that the reaction characteristics, evidenced in the first set of measurements, were not due to the quite particular acceptance of the experimental apparatus previously used.

We used in the measurements two ionization chambers with a large angular acceptance ($50° < \theta_{1,cm} < 115°, 45° < \theta_{2,cm} < 110°$) operating with an Ar-$CH_4$ gas mixture (90% Ar) at 150 mbar. Both chambers were backed by silicon surface barrier detectors to measure, at steps of 7.5°, the residual energy of the detected particles; the solid angle subtended by each SSB was 3.5 msr. Therefore twelve different angular correlations were possible between the SSBs placed at θ_1 =35°, 42.5°, 50°, 57.5° and the SSBs placed at θ_2 =−31°, −38.5°, −46° on the other side of the beam. The choice of relatively large observation angles was very effective to reject most of the two-body events originating from interactions of the beam with Carbon and Oxygen present in the target.

For both the experimental apparatus the energy resolution was $\Delta E/E \simeq 1\%$ and the charge identification was better than one charge unit up to Z-values $\simeq 22$.

3 Results

Independently from the experimental set-up, all the reactions studied show features that are similar.

In particular in the scatter plot of total measured energy ($E_1 + E_2$) versus the total measured charge ($Z_1 + Z_2$) are distinguishable three sets of events (Figs. 1a-b report data from $^{32}S+^{59}Co$ and $^{19}F+^{63}Cu$ reactions as an example): the group B due to dissipative binary processes coupled with light particle emission, the group T characterized by a large missing charge and the group C which comes from beam reactions with target contaminants.

Let us focus our attention, in the analysis, on the second set (T) of events which is distributed around $Z_1 + Z_2 \simeq 22$ for $^{19}F+^{63}Cu$ and around $Z_1 + Z_2 \simeq 28$ for the other reactions. These events are about 3÷6 % of the detected binary events and show an average value of $Z_1 + Z_2$ considerably smaller than the system atomic number. This large charge deficit ($11 < \Delta Z = Z_{projectile} + Z_{target} - (Z_1 + Z_2) < 28$, see Table 1) indicates that at least a third massive fragment was produced in the reaction, because the light particle emission alone cannot take into account of $\simeq 22$ or more emitted nucleons.

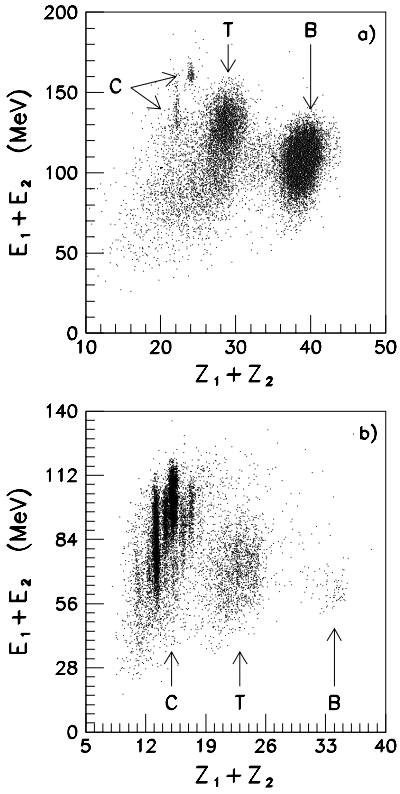

Fig. 1. Scatter plot of the total measured energy versus the total measured charge for pairs of coincident fragments detected in the reactions: **a** $^{32}S+^{59}Co$ and **b** $^{19}F+^{63}Cu$

According to this, also the relative angle between the two detected fragments (θ_{12} in Table 1) in the c.m. indicates that they are not produced in a binary process coupled to particle emission, indeed the value of θ_{12} is quite small with respect 180°. The relative small FWHM of the θ_{12} distribution (see Table 1) is a first indication that the two detected fragments are correlated; this hypothesis is also supported by the evidence of a strong charge (Figs. 2a-f) and energy (Figs. 3a-f) correlation that suggests Z_1 and Z_2 come from the decay of a single source (see [12,14,15]).

Table 1. Mean values and FWHM, in parentheses, of the experimental distributions: fragment source atomic number ($Z_s = Z_1 + Z_2$); charge deficit ($\Delta Z = Z_3$); relative angle in the c.m. of the two detected fragments (θ_{12} in deg); fragment source emission angle in the laboratory system (θ_s in deg)

SYSTEM	Z_s	ΔZ	θ_{12}	θ_s
$^{32}S+^{45}Sc$	27.0 (3.8)	11.0	144 (18)	0.13 (5.6)
$^{32}S+^{76}Ge$	27.3 (3.0)	20.7	114 (16)	0.19 (5.1)
$^{32}S+^{89}Y$	27.0 (3.4)	28.0	112 (10)	0.05 (4.2)
$^{32}S+^{59}Co$	28.5 (3.6)	14.5	144 (18)	1.83 (5.9)
$^{32}S+^{63}Cu$	28.8 (4.2)	16.2	143 (18)	1.41 (7.8)
$^{19}F+^{63}Cu$	22.5 (4.4)	15.5	139 (22)	0.75 (9.8)

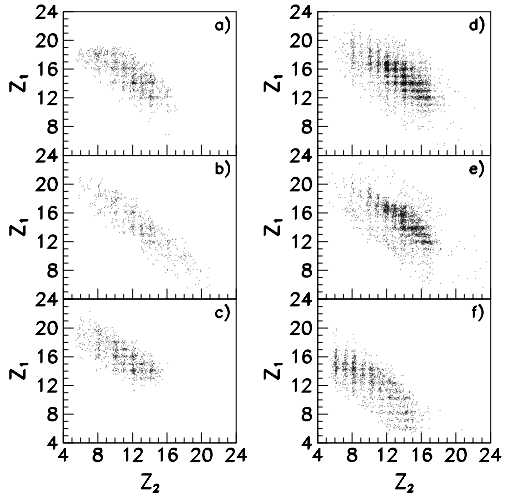

Fig. 2. Scatter plot of the atomic numbers for pairs of coincident fragments detected in three-body final states produced by the reactions: **a** ^{32}S+^{45}Sc, **b** ^{32}S+^{76}Ge, **c** ^{32}S+^{89}Y, **d** ^{32}S+^{59}Co, **e** ^{32}S+^{63}Cu and **f** ^{19}F+^{63}Cu

In Fig. 2 it looks like that the decay occurs a bit asymmetrically (with $(Z_1 - Z_2)/(Z_1 + Z_2) \simeq 0.15 \pm 0.20$) for the ^{32}S+^{45}Sc, ^{32}S+^{76}Ge and ^{32}S+^{89}Y reactions and symmetrically (with $(Z_1 - Z_2)/(Z_1 + Z_2) \simeq 0.04 \pm 0.17$) for the others. This little difference (smaller than the width of the Z-asymmetry distributions) is due to the lower acceptance of the experimental apparatus used for the first set of measurements (in Strasbourg) that introduces a weak bias in the angular correlations.

In [12] was demonstrated that the intermediate decaying complex is formed, by the projectile and part of the target transferred to it, in the first stage of a *sequential binary process*. Thus, to study of the reaction time-scale, it is important to estimate the contribution of each of the two steps and, consequently, the partition of the excitation energy between the primary fragments that has influence on their decay.

Four evidences show that the two steps of the reaction (source formation and its decay) are only weakly coupled.

i) The relative energy (E_{3s}) between the fragment source ($Z_s = Z_1 + Z_2$) and the third body (Z_3) reaches at maximum 60% of the Viola value [16] indicating that the two primary fragments are distant when Z_s decays (see Figs. 4a-f).

ii) Accordingly to this the kinetic energy of the two detected fragments, coming from the decay of Z_s, is not substantially influenced by the presence of the third body (Figs. 5a-f). In fact the final state interaction (essentially Coulomb repulsion) between the third body and the two detected fragments should increase the relative energy (E_{12}) between Z_1 and Z_2 proportionally to the size of Z_3. On the contrary E_{12}, normalized to the Viola value, does not increase with the product $Z_3 \cdot Z_s$ although, for some systems, the magnitude of this product grows significantly (up to 53% for the ^{32}S+^{45}Sc).

iii) A very little linear momentum is transferred to the third body confirming that the two primary fragments

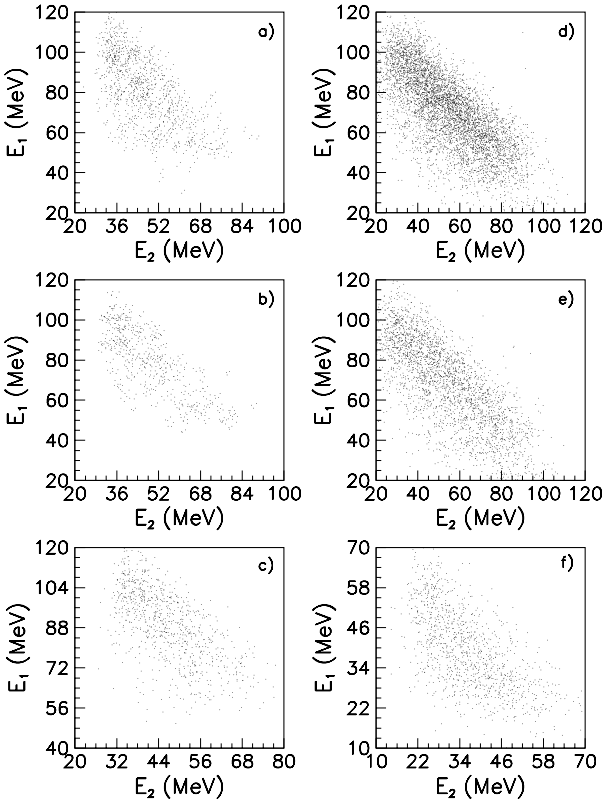

Fig. 3. Scatter plot of the kinetic energies for pairs of coincident fragments detected in three-body final states produced by the reactions: **a** ^{32}S+^{45}Sc, **b** ^{32}S+^{76}Ge, **c** ^{32}S+^{89}Y, **d** ^{32}S+^{59}Co, **e** ^{32}S+^{63}Cu and **f** ^{19}F+^{63}Cu

are only weakly interacting. This can be inferred from Figs. 6a-f in which is reported the absolute value of the vector sum ($\overline{p}_s = \overline{p}_1 + \overline{p}_2$) of the linear momenta relative to the detected fragments. We calculated the linear momenta

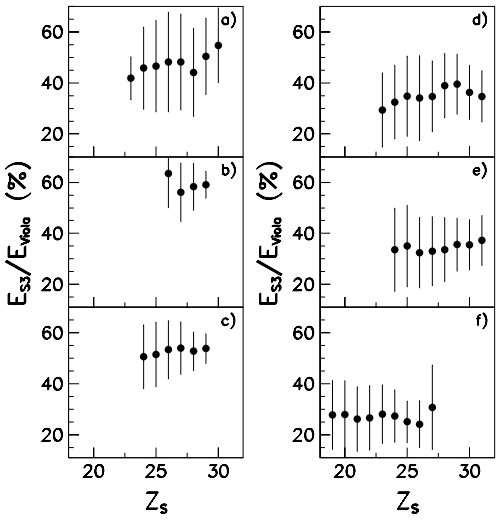

Fig. 4. Relative energy (E_{3s}) between the fragment source and the third body, in percentage of the Viola value, plotted versus the source atomic number (Z_s); the sequence of the pictures is the same than in Fig. 2

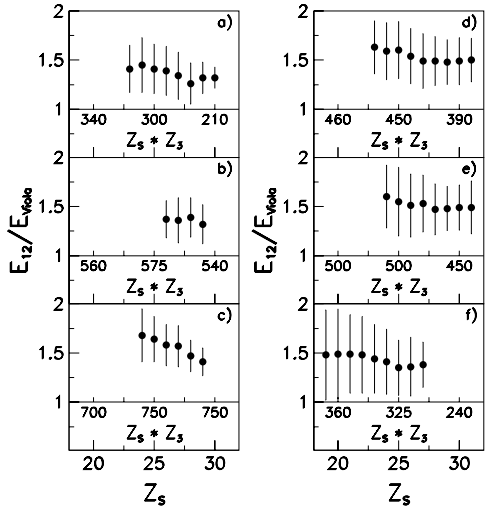

Fig. 5. Relative energy (E_{12}) between the two detected fragments (Z_1 and Z_2), normalized to the Viola value, as a function of the product $Z_3 \cdot Z_s$ of the atomic numbers of the two primary fragments; the sequence of the pictures is the same than in Fig. 2

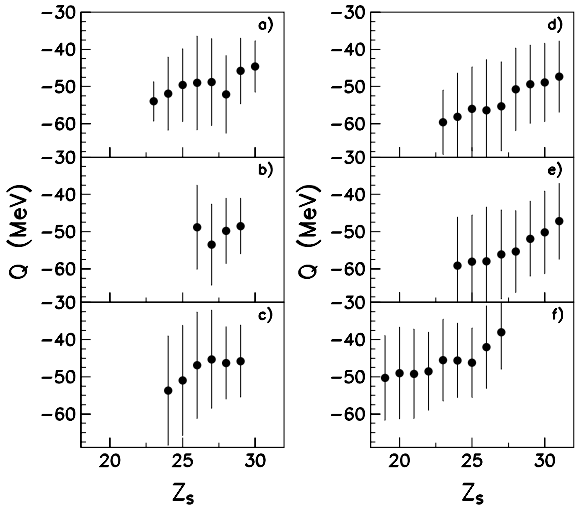

Fig. 7. Reaction Q-value plotted as a function of the source atomic number Z_s; the sequence of the pictures is the same than in Fig. 2

of the three bodies present in the final state from their kinetic energies assuming as fragment masses the minimum of the β-stability valley corresponding to the measured charges; in the calculation particle evaporation was neglected. As one can see in Figs. 6a-f the fragment source takes most of the projectile linear momentum letting the third fragment nearly at rest in the laboratory system.

iv) From the calculation of the linear momentum of the fragment source can be deduced also its emission angle. The direction of the motion of Z_s is practically parallel to the beam axis (see θ_s in Table 1). This indicates that, in the first step of the reaction the interaction, between the projectile and the target occurs without orbiting of the system in agreement with the evidence of a little linear momentum transfer. The absence of orbiting implies also that the reaction time of the first step is of the same order of magnitude of the transit-time of the projectile in the region of the target ($\simeq 5 \cdot 10^{-22}$ s).

In conclusion the four evidences previous reported indicate that the third body is the part of the target not transferred to the projectile during the interaction and that it behaves as a *weakly interacting spectator*.

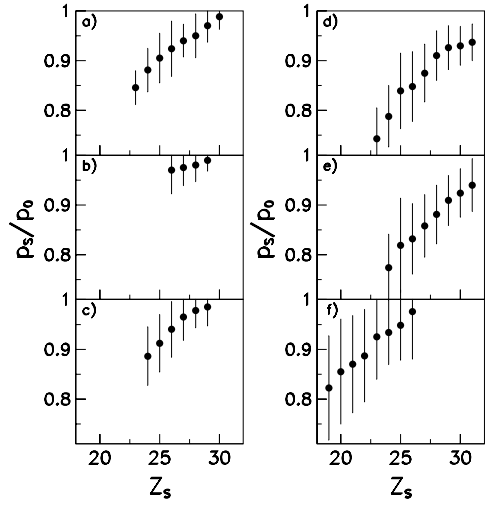

Fig. 6. Linear momentum (p_s) of the fragment source, in units of the beam momentum (p_0), plotted as a function of the source atomic number Z_s; the sequence of the pictures is the same than in Fig. 2

4 Excitation energy partition and reaction time-scale

Data analysis in terms of three-body kinematics (i.e. neglecting nucleon evaporation) allows all kinematic quantities to be determined, in particular we deduced the reaction Q-value (see Figs. 7a-f). The large inelasticity of the studied process indicates that the threshold bombarding energy is not much lower than 6 MeV$\cdot A$.

For two step binary processes in which the two primary fragments have not mutual influence on their decay, as practically it happens in our case, the second step Q-value (Q_2) can be considered approximately equal to the relative energy (E_{12}) between the secondary fragments. Therefore the second-step Q-value is a positive quantity ($Q_2 \simeq E_{12} > 0$) and only the first stage of the process is dissipative ($Q_1 < 0$), the amount of dissipated energy depending on the first step reaction mechanism.

The excitation energies of the two primary fragments (Z_s and Z_3) can be determined, by mass and energy conservation, according to:

$$E_s^* = Q_2 + S_{12} + (E_1^* + E_2^*) \quad (1)$$

$$E_3^* = Q_{ggg} - Q_1 - Q_2 - (E_1^* + E_2^*) \quad (2)$$

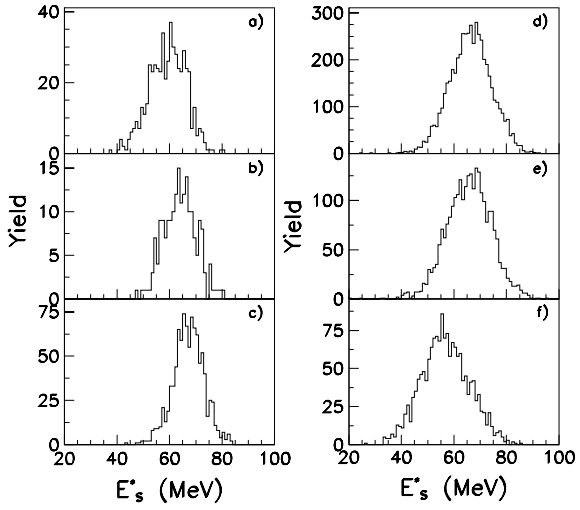

Fig. 8. Distribution of the excitation energy (E_s^*) of the fragment source (see (1)); the sequence of the pictures is the same than in Fig. 2

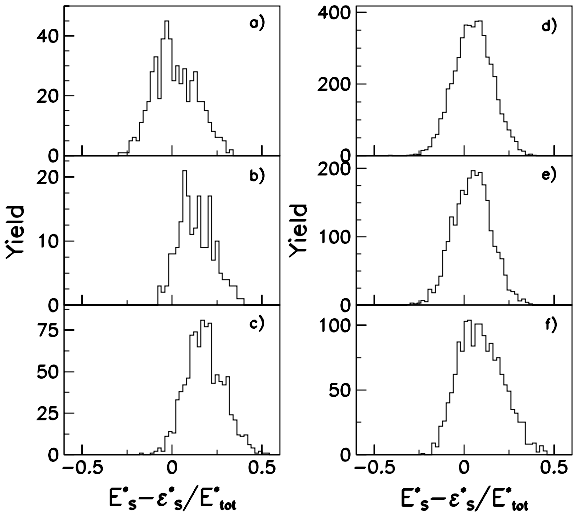

Fig. 10. Difference between the source excitation energy E_s^* (see (1)) and the value ε_s^* expected for the thermal equilibrium (see (3)) normalized to the total excitation energy E_{tot}^*; the sequence of the pictures is the same than in Fig. 2

in which E_1^* and E_2^* are the excitation energies of the two fragments produced in the source (Z_s) decay, S_{12} is the associated separation energy and Q_{ggg} is the mass difference between the entrance and the exit channel. The value of the sum $E_1^* + E_2^*$ was considered small as compared to the other terms in (1) and (2) (even as assumed at higher bombarding energies [17,18]) and then it was neglected in the calculations.

Under these assumptions the partition of the excitation energy between the primary fragments was evaluated and the results are shown in Figs. 8a-f and in Figs. 9a-f.

The width of the distributions reported in these figures suggests the presence of events with different degree of equilibration. This can be evidenced comparing E_s^* and E_3^* with the values (ε_s^* and ε_3^*) expected when the thermal equilibrium is attained. In this case the sharing of the excitation energy between the primary fragments is proportional to their masses:

$$\varepsilon_s^* = E_{tot}^* \cdot \frac{A_1 + A_2}{A_p + A_t} \tag{3}$$

$$\varepsilon_3^* = E_{tot}^* \cdot \frac{(A_p + A_t) - (A_1 + A_2)}{A_p + A_t} \tag{4}$$

where $E_{tot}^* = E_s^* + E_3^*$ is the total excitation energy, A_i is the mass of the i-th secondary fragment, A_p the mass of the projectile and A_t the mass of the target. In Figs. 10a-f is reported the difference between the excitation energy deduced from experimental data (E_s^*) and the calculated value (ε_s^*) in units of the total excitation energy (E_{tot}^*). The pictures show that, for all the studied reactions, the system is near to the thermal equilibrium because the deviation from the expectation for the largest part of events is included inside 20% of the total excitation energy; there is, however, a part of events which has excitation energy higher then that predicted by the thermal equilibrium hypothesis.

While the system is quasi-equilibrated it is reasonable to assume that the primary fragments decay by a fission-like process. Therefore we estimated the life-time of the fragment source by the formula:

$$\tau = \hbar / \Gamma_f \tag{5}$$

in which Γ_f is the width of the fission process.

It is to note that τ is the statistical-model time and that contributions to the total-fission time [19] due to dynamical effects (like the pre-saddle-delay time and the saddle-to-scission time) are not taken into account. In fact,

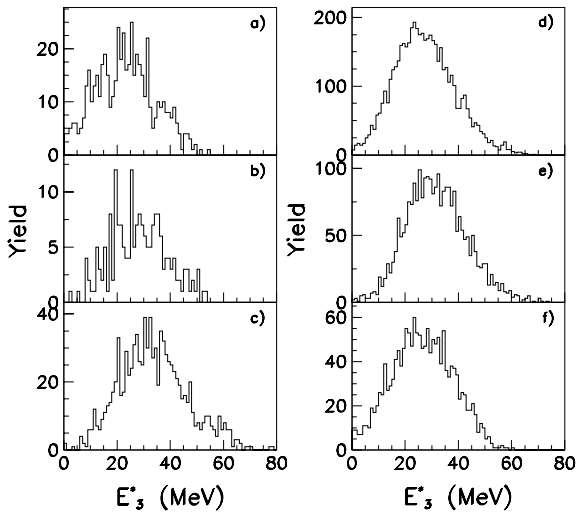

Fig. 9. Distribution of the excitation energy (E_3^*) of the third body (see (2)); the sequence of the pictures is the same than in Fig. 2

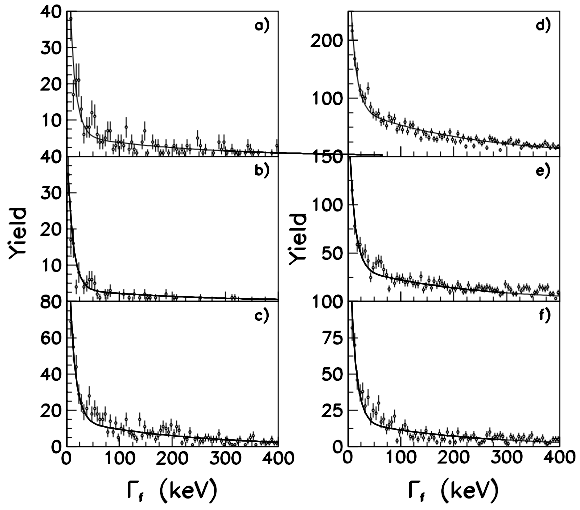

Fig. 11. Width distribution (see (6)); the *solid line* represents the best fit obtained with the sum of two exponential functions. The sequence of the pictures is the same than in Fig. 2

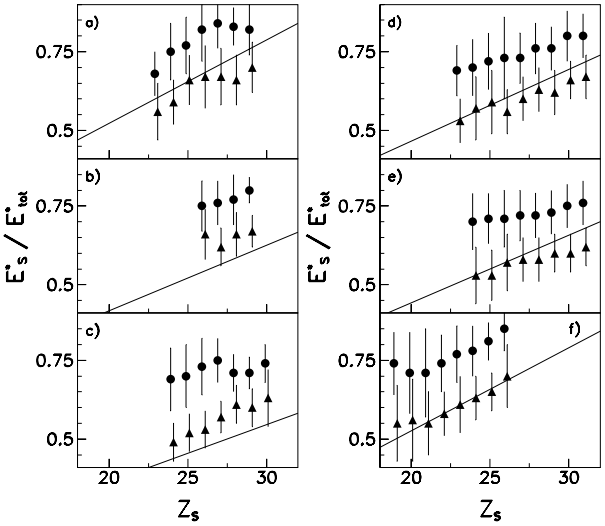

Fig. 12. Excitation energy (E^*_s) of the fragment source in unit of the total excitation energy (E^*_{tot}) as a function of the source atomic number Z_s. *Triangles* are relative to the slow-decay component ($\tau > 3.3{\cdot}10^{-20}$ s) and *points* are relative to the fast-decay component ($\tau < 3.3{\cdot}10^{-20}$ s). The *solid line* represents the expected excitation energy for the thermal equilibrium. The sequence of the pictures is the same than in Fig. 2

the contribution of the dynamical effects can be significant for heavy and medium-heavy fissioning nuclei and becomes less important for lighter nuclei like the primary fragments produced in the presently studied reactions.

In the statistical formalism [20] the different quantum states are characterized by different values of the excitation energy and of the angular momentum. Then, using the excitation energy deduced from the experimental data (see (1)), we calculated the distribution function of Γ_f for the decaying intermediate complex (the heaviest of the two primary fragments) by using the formula of [20]

$$\Gamma_f = \frac{2\sqrt{a_f(E^*_s - B_f)} - 1}{4a_f\pi \exp{(2\sqrt{a_c E^*_s})}} \cdot \exp{(2\sqrt{a_f(E^*_s - B_f)})} \quad (6)$$

In the calculation of Γ_f, we used the level density parameterization (a_c and a_f) proposed in [21] and we took into account the dynamical reduction of the fission barrier (B_f) due to the angular momentum. The values of the angular momentum can be deduced from the measured relative energy (E_{12}) of the two detected fragments. In fact E_{12} is always $\simeq$40% larger than the value predicted by the Viola systematic (E_{Viola}). This excess cannot be justified by a final state interaction between Z_3 and the detected fragments (see Figs 5a-f); consequently the additional amount of relative energy, with respect the Viola prediction, indicates the presence of a rotational motion of the breaking system ($Z_1 + Z_2$). So we determined the angular momentum of the fragment source fitting to the experimental value of E_{12} the sum of a Coulomb and a rotational term. In the fitting procedure the mutual distance between the fragments Z_1 and Z_2 was assumed equal to $d_{12} = 1.2{\cdot}(A_1^{1/3} + A_2^{1/3}) + 4$ fm and the wave was let as free parameter.

The Γ_f distribution function (Figs. 11a-f), relative to the studied systems, exhibits the clear presence of two exponential shape components. For each component it is possible to determine the average value of the width and from it, using (5), an indication of the decay time-scale of Z_s. The values obtained by a fit are: $\tau_1 \simeq 3{\cdot}10^{-21}$ s and $\tau_2 \simeq 6{\cdot}10^{-20}$ s, they do not change significantly when changing the system.

A possible explication of the different values of E^*_s experimentally observed, that give origin to two different time-scales in the decay of the fragment source, can be the partial equilibration of the excitation energy between the two primary fragments during the first step of reaction.

So we arbitrarily divided the events in two sets, the first one with $\Gamma_f > 20$ keV and then with source life-time $\tau < 3.3{\cdot}10^{-20}$ s, the second one with $\Gamma_f < 20$ keV and then with source life-time $\tau > 3.3{\cdot}10^{-20}$ s. Figs. 12a-f report, with different symbol for the two sets of events, the ratio between the excitation energy of the fragment source (E^*_s) and the total excitation energy (E^*_{tot}). This ratio is plotted as a function of Z_s and compared with the thermal equilibrium (solid line).

The events with $\Gamma_f > 20$ keV (points) have excitation energy E^*_s higher than the other ones (triangles) whose behaviour better agrees with the trend of the thermal equilibrium. Therefore it appears that in the first stage of the reaction the primary fragments can be generated with a continuum of excitation energy depending on the degree of thermalization reached by the system.

We took into account that also the light-particle emission from the intermediate complex, before of its break-up, can contribute to spread the E^*_s distribution. In this

case the source of the detected fragments (Z_1 and Z_2) should correspond to a cooled residue of the highest excited and massive primary fragment. If this happens the Z_s distribution, relative to the slow-decay component ($\tau > 3.3{\cdot}10^{-20}$ s) should be shifted at low values with respect the Z_s distribution relative to the fast-decay component ($\tau < 3.3{\cdot}10^{-20}$ s). This is expected because the intermediate complex that gives origin to Z_1 and Z_2 is highly excited and, for life time of order of τ_2, survives enough to emit some nucleons. On the contrary the Z_s distribution, relative to the slow-decay component, is not shifted at low values suggesting that the excited intermediate complex does not emit light charge particles before of its decay. Unfortunately this is not a proof but only an indication because, in our data, there is not direct information about the light-particle emission that, consequently, cannot be excluded to occur.

Any way, it is worthwhile to note that, for short life time (of order of τ_1), the prompt break-up of the fragment source makes unlike the nucleon evaporation. Therefore, particularly in this case, the different excitation energies of the decaying fragment and then the differences in its life-time seem *in primis* ruled by the reaction mechanism of the first step.

5 Conclusions

The three-body channel of the ^{32}S+^{45}Sc, ^{76}Ge, ^{89}Y, ^{59}Co, ^{63}Cu and ^{19}F+^{63}Cu reactions was studied at $\simeq 6$ MeV$\cdot A$ of incident energy.

The large amount of the energy dissipated in the process indicates that the energy threshold of this ternary process is not much lower that 60 MeV over the interaction barrier.

The three massive fragments, produced in the final state, originate in a sequential binary process in which the two steps of the reaction have very different time-scale and are only weakly coupled.

The first stage of the reaction is characterized by the transfer of about 24 nucleons from the target to the projectile to form an excited intermediate complex (the heaviest primary fragment) which decays into two secondary fragments. In the nucleon transfer from the target to the projectile only a small part of the total momentum is made over to the remaining part of the target. The partition of the excitation energy between the primary fragments was deduced by the mass and energy conservation.

Using the statistical model formalism and the excitation energy deduced from the data we calculated the fission width for the source of the secondary fragments. Two components were evidenced in the width distribution that, in the hypothesis of statistical decay of the fragment source, correspond to time-scales of $\simeq 3{\cdot}10^{-21}$ s and $\simeq 6{\cdot}10^{-20}$ s. The fast-decay component is associated to events which have only partially relaxed the excitation energy in the first step of the reaction, whereas the slow-decay component is associated to events which have reached the thermal equilibrium.

In conclusion thought the two steps of the reaction are not directly coupled, the decay of the excited intermediate complex is affected by the reaction mechanism of the first step in the sense that the excitation energy of the fragment source, and consequently its decay-time, depend on the energy equilibration in the first reaction step.

The different total mass and entrance channel asymmetry do not seem to have influence on the reaction mechanism.

References

1. Plasil, F., Ferguson, R.L., Britt, H.C., Stokes, R.H., Erkkila, B.H., Goldstone, P.D., Blann, M., Gutbrod, H.H.: Phys. Rev. Lett. **40**, 1164 (1978)
2. Tamain, B., Chechik, R., Fuchs, H., Hanappe, F., Morjean, M., Ngô, C., Peter, J., Dakowski, M., Lucas, B., Mazur, C., Ribrag, M., Signarbieux, C.: Nucl. Phys. A **330**, 253 (1979)
3. Eyal, Y., Gavron, A., Tserruya, I., Fraenkel, Z., Eisen, Y., Wald, S., Bass, R., Gould, G.R., Kreyling, G., Renfordt, R., Stelzer, K., Zitzmann, R., Gobbi, A., Lynen, U., Stelzer, H., Rode, I., Bock, R.: Phys. Rev. Lett. **41**, 625 (1978)
4. Hilscher D., Birkelund, J.R., Hoover, A.D., Schröder, W.U., Wilcke, W.W., Hiuzenga, J.R., Mignerey, A.C., Wolf, K.L., Breuer, H.F., Viola, V.E. Jr.: Phys. Rev. C **20**, 576 (1979)
5. Tserruya, I., Breskin, A., Chechik, R., Fraenkel, Z., Wald, S., Zwang, N., Bock, R., Dakowski, M., Gobbi, A., Sann, H., Bass, R., Kreyling, G., Renfordt, R., Stelzer, K., Arlt, U.: Phys. Rev. C **26**, 2509 (1982)
6. Vandenbosch, R., Lazzarini, A., Leach, D., Lock, D.K., Ray, A., Seamster, A.: Phys. Rev. Lett. **52**, 1964 (1984)
7. Awes, T.C., Ferguson, R.L., Novotny, R., Obenshain, F.E., Plasil, F., Pontoppidan, S., Rauch, V., Young, G.R., Sann, H.: Phys. Rev. Lett. **52**, 251 (1984)
8. Randrup, J.: Nucl. Phys. A **327**, 490 (1979)
9. Feldmeier, H., Spangenberger, H.: Nucl. Phys. A **428**, 223c (1984)
10. Randrup, J.: Nucl. Phys. A **383**, 468 (1982)
11. Moretto, L.G.: Z. Phys. A **310**, 61 (1983)
12. Boccaccio, P., Bettiolo, M., Doná, R., Vannucci, L., Ricci, R.A., Vannini, G., Massa, I., Coffin, J.P., Fintz, P., Guillaume, G., Jundt, F., Rami, F., Wagner, P.: Z. Phys. A **354**, 121 (1996)
13. Vannucci, L., Boccaccio, P., Ricci, R.A., Vannini, G., Doná, R., Massa, I., Coffin, J.P., Fintz, P., Guillaume, G., Jundt, F., Rami, F., Wagner, P.: Proceedings of the International Symposium on Large-Scale Collective Motion of Atomic Nuclei, October 15-19, 1996, Brolo, Italy.
14. Vannini, G., Massa, I., Lavagnini, L., Boccaccio, P., Vannucci, L., Ricci, R.A., Iori, I., Coffin, J.P., Fintz, P., Gonin, M., Guillaume, G., Heusch, B., Jundt, F., Malki, A., Rami, F., Wagner, P.: Europhys. Lett. **7**, 311 (1988)
15. Boccaccio, P., Mwose, P.K., Vannucci, L., Bettiolo, M., Ricci, R.A., Augustyniak, W., Massa, I., Vannini, G., Coffin, J.P., Fintz, P., Guillaume, G., Heusch, B., Jundt, F., Rami, F., Wagner, P.: Il Nuovo Cimento A **106**, 379 (1993)

16. Viola, V.E., Kwiatkowski, K., Walker, M.: Phys. Rev. C **1550**, 31 (1985)
17. Stern, M.,Billerey, R., Chambon, B., Chbihi, A., Chevarier, A., Chevarier, N., Cheynis, B., Drain, D., Pastor, C., Alarja, J., Dauchy, A., Giorni, A., Heuer, D., Morand, C., Viano, J.B.: Z. Phys. A **331**, 323 (1988)
18. Schmidt, H.R., Gazes, S.B., Chan, Y., Kamermans, R., Stokstad, R.G.: Phys. Lett. B **180**, 9 (1986)
19. Hinde, D.J., Hilscher, D., Rossner, H., Gebauer, B., Lehmann, M., Wilpert, M.: Phys. Rev. C **45**, 1229 (1992)
20. Huizenga, J.R. and Vandenbosch, R.: In: Nuclear Reactions, Endt, P.M. and Smith P.B. (eds.), vol II, p. 47. Amsterdam: North-Holland Publishing Company 1962
21. D'Arrigo, A., Giardina, G., Herman, M., Ignatyuk, A.V., Taccone, A.: Jou. of Phys. G **20**, 365 (1994)